Realistic numerical modelling of head tissues exposure to electromagnetic waves from mobile phones

O. Clatz[1] S. Lanteri[2] S. Oudot[3] J.P Pons[4]
S. Piperno[5] G. Scarella[2] J. Wiart[6]

[1]INRIA, project-team EPIDAURE
[2]INRIA, project-team CAIMAN
[3]INRIA, project-team GÉOMETRICA
[4]INRIA, project-team ODYSSÉE
[5]INRIA/CERMICS, project-team CAIMAN

2004 Route des Lucioles, BP 93
06902 Sophia Antipolis Cedex, France

[6]France Telecom R&D, IOP team, 38-40 rue du General Leclerc
92794 Issy-Les-Moulineaux Cedex 9, France

Symposium Telius, STIC et Santé
HP European Technical Center, Sophia Antipolis, June 12th 2006

Content

1. Electromagnetic waves and humans
2. Exposure to mobile phone radiation
3. Numerical dosimetry of EM fields
4. HeadExp collaborative research action
5. Ongoing and future works

ElectroMagnetic (EM) waves and humans

- EM waves are increasingly present in our daily environment
  - Natural sources (earth magnetic field, etc.)
  - Manmade sources
    - Domestic appliances: TV, radio, microwave ovens, hairdryers, fridges, etc.
    - Technological devices: mobile phones, Wi-Fi, etc.
- Electromagnetic fields
  - An EM field is characterized by its frequency (Hz, MHz, GHz)
  - Ionising radiation
    - Upper part of the frequency spectrum
    - Can induce changes at the molecular level
    - x-rays and gamma rays
  - Non-ionising radiation
    - Lower part of the frequency spectrum
    - Static and power frequency fields, radiofrequencies, microwaves and infrared radiation

ElectroMagnetic (EM) waves and humans

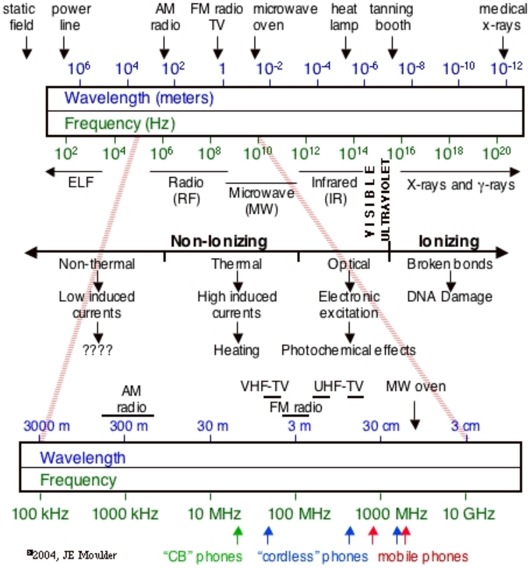

ElectroMagnetic (EM) waves and humans

- Effects of radiofrequencies (RF) and microwaves (MW) on humans
  - Energy from RF and MW is absorbed into the body

$$\text{SAR (Specific Absorption Rate)} : \frac{\sigma|\mathbf{E}|^2}{\rho}$$

    - $\mathbf{E}$: electric field
    - σ: tissue conductivity
    - ρ: tissue density
  - Energy is converted to heat
  - Energy is dissipated by the body's normal thermoregulatory process
- No evidence that exposure to RF and MW is harmful
- Guidelines have been produced by a number of bodies around the world
  - National Radiological Protection Board (NRPB)
  - International Commission for Non-Ionising Radiation Protection (ICNIRP)

Exposure to mobile phone radiation

- Health issues related to hand-held mobile phones
  - J.E. Moulder, K.R. Foster, L.S. Erdreich, J.P. McNamee: Mobile phones, mobile phone base stations, and cancer: a review. Int. J. Rad. Biol., 2005.
  - 2000-2001 review by the Royal Society of Canada
  - 2000 report of the UK Independent Expert Group on Mobile Phones (the "Stewart Commission")
  - Human exposure to radio frequency and microwave radiation from portable and mobile telephones and other wireless communication devices. A COMAR[1] technical information statement. IEEE Eng. Med. Biol., 2001.
  - 2001 review from the World Health Organization
  - 2001 review from American Cancer Society
  - 2002 report from the Health Council of the Netherlands
  - Reviews from the UK NRPB in 2003-2005
- FAQs by J. Moulder on health and safety issues related to EM fields http://www.mcw.edu/gcrc/cop/cell-phone-health-FAQ/toc.html

[1] IEEE Committee on Man and Radiation

Exposure to mobile phone radiation

- Health issues related to hand-held mobile phones
  - Rapport Zmirou, Direction Générale de la Santé, 2001
    http://www.sante.gouv.fr/htm/dossiers/telephon_mobil/rapport_zmirou.htm
  - Etude INERIS (Institut National de l'Environnement industriel et des RISques) bibliographique sur la problématique fréquences et santé
    http://www.art-telecom.fr/publications/index-etud-ineris.htm
  - Rapport de l'OPECST (Office Parlementaire d'Evaluation des Choix Scientifiques et Technologiques du Sénat) n 52, 2002-2003
    http://www.senat.fr/rap/r02-052/r02-052.html
  - Rapport de l'AFSSE (Agence Française de Sécurité Sanitaire de l'Environnement et du Travail), 2005
    http://www.afsse.fr/documents/rapport_telephonie_mobile_2005.pdf

Exposure to mobile phone radiation

- Health issues related to hand-held mobile phones
  - Biological effects versus sanitary effects
    - Biological effects: physiological, biochemical or behavioral changes induced in a body, tissue or cell by an external source
    - A biological effect does not necessarily represent a risk for human health
    - Sanitary effects: consequences of biological effects that change the normal behavior of a body
  - Thermal effects versus non-thermal effects
    - A thermal effect results from a local or systemic heatinc of a tissue
    - Thermal effects are relatively well known
    - Ongoing studies are concerned with non-thermal effects

Exposure to mobile phone radiation

- Health issues related to hand-held mobile phones
  - Epidemiological studies
    - Possible links with various cancers
  - Experimental studies
    - Dosimetry of animal exposure
    - In vivo and in vitro studies
  - Computer simulation studies
    - Numerical dosimetry of EM fields
    - Evaluation of temperature elevation in tissues

Numerical dosimetry of EM fields

- Numerical dosimetry in biological tissues can be used for:
  - compliance testing,
  - understanding the underlying physical mechanisms,
  - planning purposes and design objectives (medical applications).
- Numerical modelling aims at providing:
  - the dosimetry of the electromagnetic radiation (SAR distribution),
  - the temperature elevation of tissues,
  - optimization of the treatment (electrode shape design, antenna configuration, etc.).
- Numerical modelling requires geometrical models:
  - built from medical images,
  - must describe several tissues (e.g muscle, blood, bone, etc.),
  - should be suited to localized discretization strategies.

$$\left\{\begin{array}{rcccl} \varepsilon(\mathbf{x})\dfrac{\partial \mathbf{E}}{\partial t} & - & \nabla \times \mathbf{H} & = & -\mathbf{J} \\ \mu(\mathbf{x})\dfrac{\partial \mathbf{H}}{\partial t} & + & \nabla \times \mathbf{E} & = & 0 \end{array}\right.$$

- $\mathbf{E} = \mathbf{E}(\mathbf{x}, t)$: electric field
- $\mathbf{H} = \mathbf{H}(\mathbf{x}, t)$: magnetic field
- $\varepsilon(\mathbf{x})$: electric permittivity
- $\mu(\mathbf{x})$: magnetic permeability
- $\mathbf{J} = \mathbf{J}(\mathbf{x}, t)$: electric current density
    - Conductive media: $\mathbf{J} = \sigma \mathbf{E}$
    - $\sigma(\mathbf{x})$: electric conductivity

Numerical dosimetry of EM fields

Numerical methods on uniform, cartesian grids

- FDM: Finite Difference Methods
- Advantages
  - Easy computer implementation
  - Computationally efficient (very low algorithmic complexity)
  - Mesh generation is straightforward (medical images are voxel based)
  - Modelization of complex sources (antennas, thin wires, etc.) is well established
- Drawbacks
  - Accuracy on non-uniform discretizations
  - Memory requirements for high resolution models
  - Approximate discretization of boundaries (stair case representation)
- Numerical dosymetry analysis of mobile phones radiation most often relies on the FDTD method
  - P. Bernardi *et al.* (U. La Sapienza, Roma, Italy)
  - O.P. Gandhi *et al.* (U. of Utah, USA)
  - J. Wiart *et al.* (FTR&D, France)
  - etc.

Numerical dosimetry of EM fields

Numerical methods on non-uniform grids

- FEM: Finite Element Methods
- FVM: Finite Volume Methods
- Advantages
  - Accurate representation of surfaces (e.g interfaces between tissues)
  - Amenable to local refinment strategies
  - Well suited to high order interpolation methods
  - Flexibility with regards to heterogeneity (e.g discontinuous Galerkin methods)
- Drawbacks
  - Computer implementation is less trivial
  - Computing time
  - Unstructured mesh generation is hardly automated
  - Continuous finite element solvers are implicit (mass matrix)
- Related works
  - P. Wainwright and P. Dimbylow (Health Protection Agency, UK)
  - FEKO commercial software, hybrid Mom/FEM (South Africa)

Numerical dosimetry of EM fields

- ε, σ and ρ are varying from one tissue to the other
- They also depend on the frequency of the signal
- Discontinuities of **E** and **H** occur at interfaces between different tissues

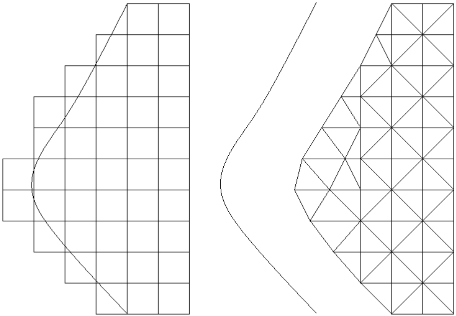

FDM **FEM/FVM**

Discontinuous Galerkin methods

- Initially introduced to solve neutron transport problems (Reed and Hill, 1973)
- Became popular as a framework for solving hyperbolic or mixed hyperbolic/parabolic problems
- Recently developed for elliptic problems
- Somewhere between a finite element and a finite volume method, gathering many good features of both
- Main properties
  - Can easily deal with discontinuous coefficients and solutions
  - Can handle unstructured, non-conforming meshes
  - Yield local finite element mass matrices
  - High-order accurate methods with compact stencils
  - Naturally adapted to *p*-adaptivity
  - Amenable to efficient parallelization

$\mathbb{P}_k$-DGTD formulation for Maxwell equations

- Tetrahedral meshes
- Centered fluxes, leap-frog time integration
- Bernacki, Fezoui, Lanteri and Piperno, J. Comput. Acoust. 2006

$$\left\{\begin{array}{lcl}
\displaystyle\iiint_{\tau_i} \vec{\varphi}\cdot\varepsilon_i \frac{\mathbf{E}_i^{n+1}-\mathbf{E}_i^{n}}{\Delta t}\,d\omega & = & \displaystyle -\sum_{k\in\mathcal{V}_i}\Phi_{H,ik}^{n+\frac{1}{2}} + \iiint_{\tau_i}\nabla\times\vec{\varphi}\cdot\mathbf{H}_i^{n+\frac{1}{2}}\,d\omega \\
\displaystyle\iiint_{\tau_i} \vec{\varphi}\cdot\mu_i \frac{\mathbf{H}_i^{n+\frac{3}{2}}-\mathbf{H}_i^{n+\frac{1}{2}}}{\Delta t}\,d\omega & = & \displaystyle \sum_{k\in\mathcal{V}_i}\Phi_{E,ik}^{n+1} - \iiint_{\tau_i}\nabla\times\vec{\varphi}\cdot\mathbf{E}_i^{n+1}\,d\omega
\end{array}\right.$$

$$\text{with :}\quad \left\{\begin{array}{lcl}
\Phi_{H,ik}^{n+\frac{1}{2}} & = & \displaystyle\iint_{a_{ik}}\vec{\varphi}\cdot\frac{\mathbf{H}_i^{n+\frac{1}{2}}+\mathbf{H}_k^{n+\frac{1}{2}}}{2}\times\vec{n}_{ik}\,d\sigma \\
\Phi_{E,ik}^{n+1} & = & \displaystyle\iint_{a_{ik}}\vec{\varphi}\cdot\frac{\mathbf{E}_i^{n+1}+\mathbf{E}_k^{n+1}}{2}\times\vec{n}_{ik}\,d\sigma
\end{array}\right.$$

$\mathbb{P}_k$-DGTD formulation for Maxwell equations

$$\mathbf{E}_i^n(\mathbf{x}) = \sum_{1\leq j\leq d_i} E_{ij}^n \vec{\varphi}_{ij}(\mathbf{x}) \ \text{ and } \ \mathbf{H}_i^{n+\frac{1}{2}}(\mathbf{x}) = \sum_{1\leq j\leq d_i} H_{ij}^{n+\frac{1}{2}} \vec{\varphi}_{ij}(\mathbf{x})$$

- $\mathbb{E}_i^n = \{E_{ij}^n\}_{1\leq j\leq d_i}$ and $\mathbb{H}_i^{n+\frac{1}{2}} = \{H_{ij}^{n+\frac{1}{2}}\}_{1\leq j\leq d_i}$
- $M_i^\varepsilon = \varepsilon_i \iiint_{\tau_i} {}^{\mathsf{T}}\vec{\varphi}_{ij}\vec{\varphi}_{ij} d\omega$ and $M_i^\mu = \mu_i \iiint_{\tau_i} {}^{\mathsf{T}}\vec{\varphi}_{ij}\vec{\varphi}_{ij} d\omega$

$$1 \leq j \leq d_i \quad : \quad \left\{ \begin{array}{rl} \left[M_i^\varepsilon \dfrac{\mathbb{E}_i^{n+1} - \mathbb{E}_i^n}{\Delta t} \right]_j & = -\displaystyle\sum_{k\in\mathcal{V}_i} \Phi_{H,ik}^{n+\frac{1}{2}} + \iiint_{\tau_i} \nabla \times \vec{\varphi}_{ij} \cdot \mathbf{H}_i^{n+\frac{1}{2}} d\omega \\ \left[M_i^\mu \dfrac{\mathbb{H}_i^{n+\frac{3}{2}} - \mathbb{H}_i^{n+\frac{1}{2}}}{\Delta t} \right]_j & = \displaystyle\sum_{k\in\mathcal{V}_i} \Phi_{E,ik}^{n+1} - \iiint_{\tau_i} \nabla \times \vec{\varphi}_{ij} \cdot \mathbf{E}_i^{n+1} d\omega \end{array} \right.$$

Computer implementation aspects

- Unstructured tetrahedral meshes
- $\mathbb{P}_0$-DGTD: finite volume solver
  - 6 dof per tetrahedron
  - CFL=1
- $\mathbb{P}_1$-DGTD: DG based on linear interpolation
  - Nodal (Lagrange) basis functions
  - 24 dof per tetrahedron
  - CFL=$\frac{1}{3}$
- SPMD parallelization strategy
  - Mesh partitioning (ParMeTiS)
  - Message passing programming model (MPI)

HeadExp collaborative research action

HeadExp realistic numerical modelling of human HEAD tissues EXPosure to electromagnetic waves radiation from mobile phones

- A multi-disciplinary cooperative research action
  - From January 2003 to December 2004
  - Partners: INRIA (CAIMAN, EPIDAURE, GAMMA, ODYSSÉE, ONDES), ENST Paris, INERIS et FT R&D
- Objectives
  - Contribute to ongoing research activities on biological effects resulting from the use of mobile phones
  - Demonstrate the benefits of using unstructured mesh Maxwell solvers for numerical dosimetric studies
  - Evaluate the thermal effects induced by the electromagnetic radiation in head tissues
- Specific activities
  - Medical image processing (segmentation of head tissues)
  - Geometrical modelling (surface and volumic mesh generation)
  - Numerical modelling (time domain Maxwell solvers, bioheat equation solver)
  - Experimental validations

HeadExp collaborative research action

Characteristics of tissues (F=1800 MHz)

Tissue	ε_r	σ (S/m)	ρ (Kg/m^3)	λ (mm)
Skin	43.85	1.23	1100.0	26.73
Skull	15.56	0.43	1200.0	42.25
CSF	67.20	2.92	1000.0	20.33
Brain	43.55	1.15	1050.0	25.26

- Geometrical models
  - Built from segmented medical images
  - Collaboration with INRIA teams specialized in medical image processing and geometrical modelling
  - Extraction of surfacic (triangular) meshes of the tissue interfaces using specific tools
    - Marching cubes + adaptive isotropic surface remeshing (P. Frey, 2001)
    - Delaunay refinement (J.-D. Boissonnat and S. Oudot, 2005)
    - Level-set method (J.-P. Pons, 2005)
  - Generation of tetrahedral meshes using a Delaunay/Voronoi tool

HeadExp collaborative research action

Characteristics of unstructured meshes of head tissues

- Coarse mesh (M1)
  - # vertices: 135,633 and # tetrahedra: 781,742

Tissue	L_{min} (mm)	L_{max} (mm)	L_{moy} (mm)	λ (mm)
Skin	1.339	8.055	4.070	26.73
Skull	1.613	7.786	4.069	42.25
CSF	0.650	7.232	4.059	20.33
Brain	0.650	7.993	4.009	25.26

- Fine mesh (M2)
  - # vertices: 889,960 and # tetrahedra: 5,230,947

Tissue	L_{min} (mm)	L_{max} (mm)	L_{moy} (mm)	λ (mm)
Skin	0.821	5.095	2.113	26.73
Skull	0.776	4.265	2.040	42.25
CSF	0.909	3.701	1.978	20.33
Brain	0.915	5.509	2.364	25.26

Surfacic meshes (mesh M1)

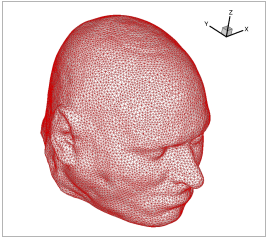

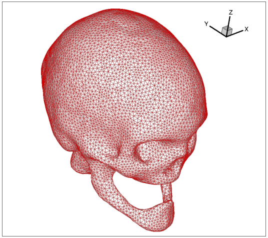

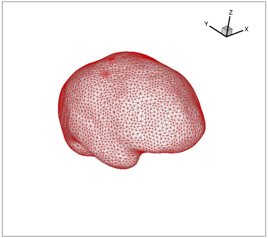

HeadExp collaborative research action

Surfacic meshes (mesh M2)

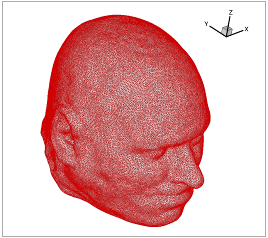

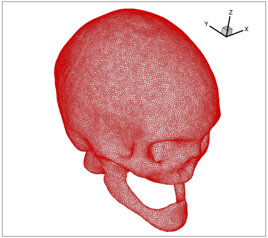

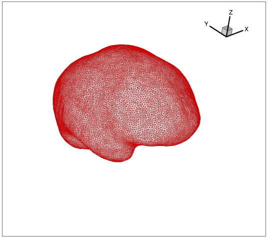

HeadExp collaborative research action

Head + simplified telephone model

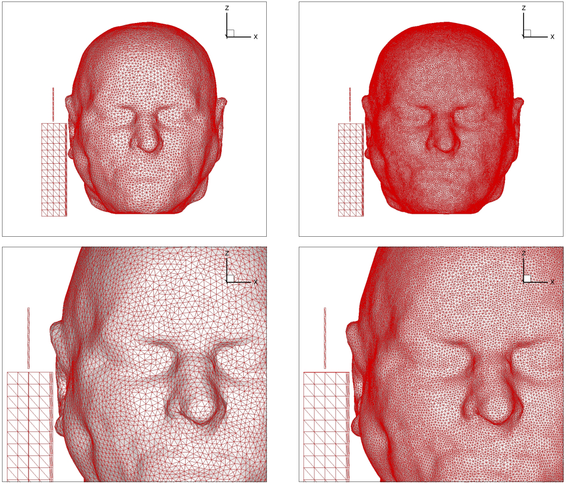

HeadExp collaborative research action

Characteristics of unstructured meshes
Head tissues + telephone + freespace

- Coarse mesh (M1)
  - # vertices: 311,259 and # tetrahedra: 1,862,136
  - Time step: 0.653 psec ($\mathbb{P}_0$-DGTD method) and 0.019 psec ($\mathbb{P}_1$-DGTD method)

L_{min} (mm)	L_{max} (mm)	L_{moy} (mm)
0.650	8.055	4.064

- Fine mesh (M2)
  - # vertices: 1,308,842 and # tetrahedra: 7,894,172
  - Time step: 0.663 psec ($\mathbb{P}_0$-DGTD method)

L_{min} (mm)	L_{max} (mm)	L_{moy} (mm)
0.776	5.509	2.132

HeadExp collaborative research action

SAR (Specific Absorption Rate) : $\dfrac{\sigma|\mathbf{E}|^2}{\rho}$

SAR/SARmax (log scale)

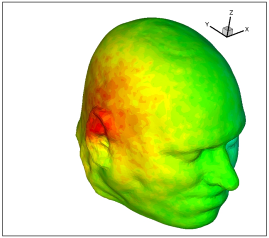

Mesh M1, $\mathbb{P}_0$-DGTD method

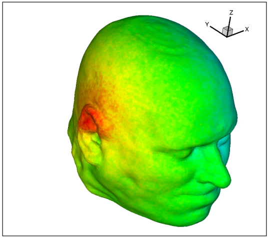

Mesh M2, $\mathbb{P}_0$-DGTD method

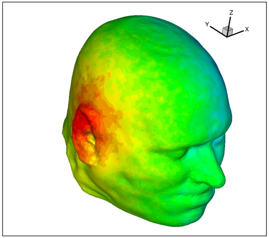

Mesh M1, $\mathbb{P}_1$-DGTD method

SAR (Specific Absorption Rate) : $\dfrac{\sigma|\mathbf{E}|^2}{\rho}$

SAR/SARmax (log scale)

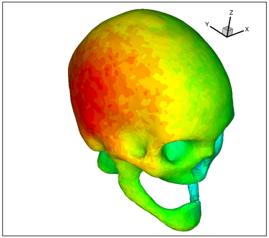

Mesh M1, $\mathbb{P}_0$-DGTD method

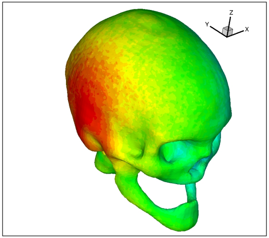

Mesh M2, $\mathbb{P}_0$-DGTD method

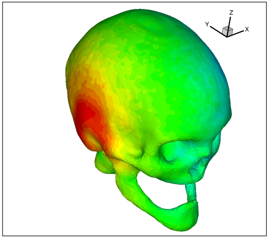

Mesh M1, $\mathbb{P}_1$-DGTD method

HeadExp collaborative research action

SAR (Specific Absorption Rate) : $\dfrac{\sigma|\mathbf{E}|^2}{\rho}$

SAR/SARmax (log scale)

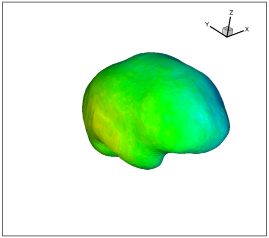

Mesh M1, $\mathbb{P}_0$-DGTD method

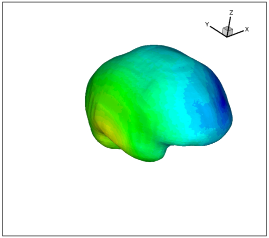

Mesh M2, $\mathbb{P}_0$-DGTD method

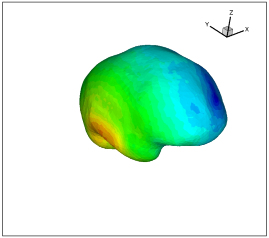

Mesh M1, $\mathbb{P}_1$-DGTD method

HeadExp collaborative research action

Electric field amplitude $|\mathbf{E}|$ (log sacle)

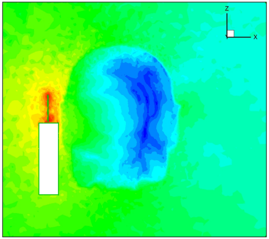

Mesh M1, $\mathbb{P}_0$-DGTD method

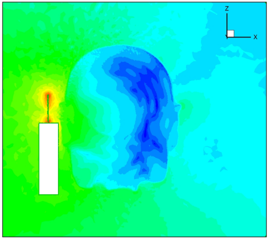

Mesh M2, $\mathbb{P}_0$-DGTD method

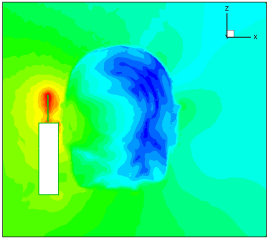

Mesh M1, $\mathbb{P}_1$-DGTD method

SAR (Specific Absorption Rate) : $\dfrac{\sigma|\mathbf{E}|^2}{\rho}$

SAR 1g/PTOT

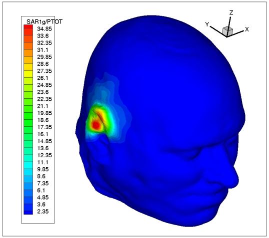

Mesh M1, $\mathbb{P}_0$-DGTD method

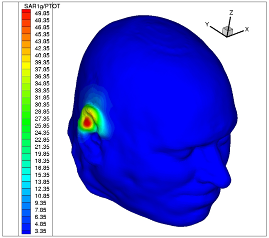

Mesh M2, $\mathbb{P}_0$-DGTD method

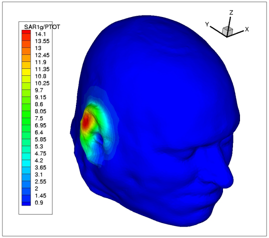

Mesh M1, $\mathbb{P}_1$-DGTD method

HeadExp collaborative research action

SAR (Specific Absorption Rate) : $\dfrac{\sigma|\mathbf{E}|^2}{\rho}$

SAR 10g/PTOT

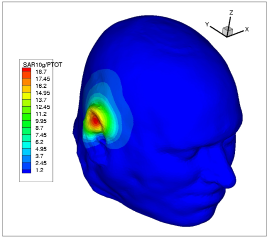

Mesh M1, $\mathbb{P}_0$-DGTD method

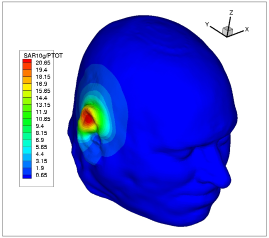

Mesh M2, $\mathbb{P}_0$-DGTD method

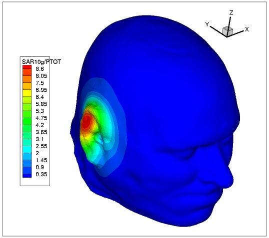

Mesh M1, $\mathbb{P}_1$-DGTD method

HeadExp collaborative research action

Mesh	Method	Local SAR (W/Kg)	SAR_{1g} (W/Kg)	SAR_{10g} (W/Kg)
M1	$\mathbb{P}_0$-DGTD	104.3	37.7	19.5
-	$\mathbb{P}_1$-DGTD	23.8	15.0	9.1
M2	$\mathbb{P}_0$-DGTD	309.9	53.8	22.4

Normalized peak SAR values

Mesh	Mehod	N_p	CPU	REAL	% CPU	$S(N_p)$
M1	$\mathbb{P}_0$-DGTD	32	36 mn	39 mn	92%	-
-	$\mathbb{P}_1$-DGTD	32	6 h 32 mn	6 h 48 mn	95%	-
M2	$\mathbb{P}_0$-DGTD	32	2 h 46 mn	2 h 54 mn	95%	1.00
-	-	64	1 h 20 mn	1 h 25 mn	94%	2.00

Cluster of AMD Opteron/2.0 GHz nodes, Gigabit Ethernet

Ongoing and future works

- Temperature elevations in tissues

$$\rho C \frac{\partial T}{\partial t} = \nabla.(\kappa \nabla T) - \beta(T - T_a) + Q_m + Q_{ext}$$

  - External source term: $Q_{ext}(\mathbf{x}, t) = \rho(\mathbf{x}, t)\mathrm{SAR}(\mathbf{x}, t)$

- Geometrical modelling
  - Local refinement strategies
  - Simultaneous extraction of surfacic meshes for several tissue interfaces
  - Non-conforming tetrahedral meshes

- Numerical modelling
  - High-order $\mathbb{P}_k$-DGTD methods
  - k-adaptivity

THANK YOU FOR YOUR ATTENTION!

Ongoing and future works

- Temperature elevations in tissues

$$\rho C \frac{\partial T}{\partial t} = \nabla.(\kappa \nabla T) - \beta(T - T_a) + Q_m + Q_{ext}$$

  - External source term: $Q_{ext}(\mathbf{x}, t) = \rho(\mathbf{x}, t)\mathrm{SAR}(\mathbf{x}, t)$

- Geometrical modelling
  - Local refinement strategies
  - Simultaneous extraction of surfacic meshes for several tissue interfaces
  - Non-conforming tetrahedral meshes

- Numerical modelling
  - High-order $\mathbb{P}_k$-DGTD methods
  - k-adaptivity

THANK YOU FOR YOUR ATTENTION!